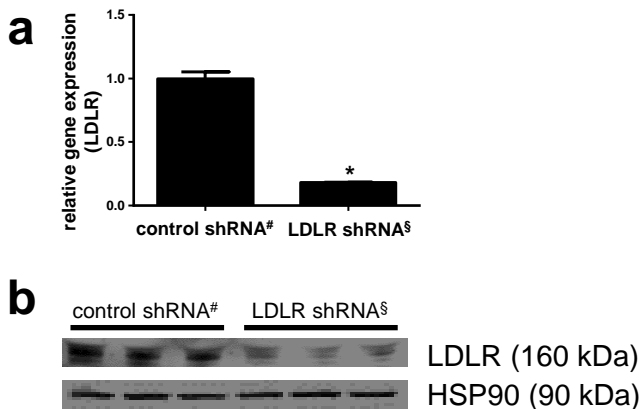


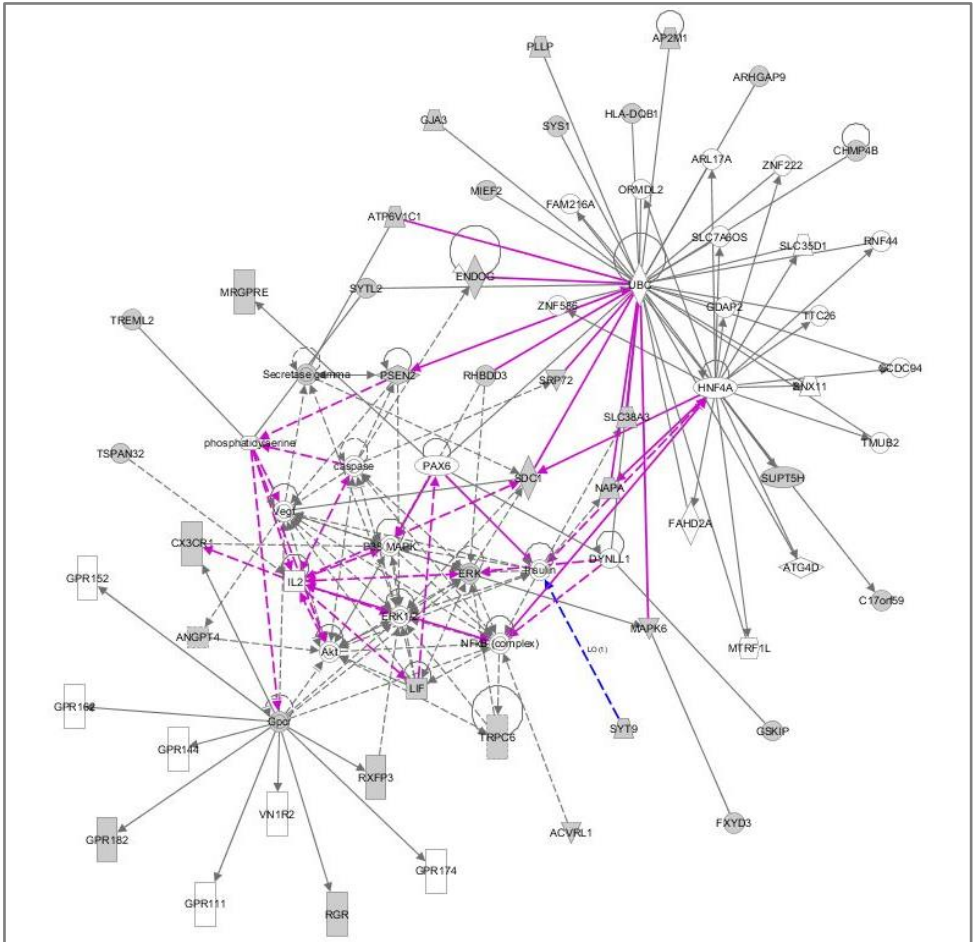
# Supplementary Figure 1



## Supplementary Fig. 1. EA.hy926 cell line with LDLR knockdown.

a) qPCR result for EA.hy926 transduced with either scramble shRNA lentivirus or the 5 shRNA lentiviruses targeting the ORF of LDLR. #, cells cultured in LPDS. §, cells cultured in LDL supplemented media (25  $\mu\text{g}/\text{ml}$ ). Data represent the mean  $\pm$  SEM and are representative of 3 experiments in duplicate. \* $p < 0.05$ , Student's t-test. b) Western blot analysis for EA.hy926 transduced with either scramble shRNA lentivirus or the 5 shRNA lentiviruses targeting the ORF of LDLR. #, cells cultured in LPDS. §, cells cultured in LDL-supplemented media (25  $\mu\text{g}/\text{ml}$ ) A non-cropped western blot for this experiment can be found in Supplementary Figure 11b.

# Supplementary Figure 2



**Supplementary Fig. 2. Qiagen's Ingenuity Pathway Analysis.**  
Analysis of the 34 gene hits revealed 3 distinct networks. Representation in a gene cluster format.

# Supplementary Figure 3

Gene symbol	E+T+H+L+S					CVD	Lipids	Gene symbol	E+T+H+L+S					CVD	Lipids	Gene symbol	E+T+H+L+S					CVD	Lipids								
	E	T	H	L	S				E	T	H	L	S				E	T	H	L	S			E	T	H	L	S			
ABCC8	1	2	1	1	0			GLCT	1	2	1	1	0		MAE241	1	2	1	1	0			SDPR	1	1	1	1	0			
ABCF1	0	2	1	0	0			GLMN	1	1	0	1	1	0		MAE241	3	2	4	2	2			SDPR	1	1	1	1	0		
ABCG5	2	2	1	1	0		CAD	COG1	1	1	3	2	0		MAE241	2	1	2	0	2			SDPR	1	0	2	0	2			
ABHD12B	1	2	2	0	1			CRELD1	0	1	1	1	2		MAE241	1	0	1	4	0			SDPR	1	0	2	0	2			
ACVPL1	4	1	4	0	1			CSNK1E	1	0	1	2	0		MAE241	3	2	2	0	0			SDPR	0	1	0	0	0			
ADORA1	1	1	2	0	0			CDC81	2	1	1	3	0		MARCKE	2	0	4	0	0			SDPR	0	2	0	0	0			
ANGPT4	2	1	4	0	0			CX4668	0	1	1	1	1		MARCKE	1	1	4	0	0			SDPR	1	0	1	1	1			
ANGPT2	2	4	1	0	0			DOCK6	0	1	1	1	1		MAP4	4	0	1	4	0			SDPR	1	0	1	1	1			
AP2M1	2	0	4	0	0		SBP, DBP, MAP	DPH4	0	1	1	0	1		ND1	0	1	1	0	0			SDPR	0	1	1	0	0			
APOB	0	2	0	0	0			DPVSL2	0	1	2	4	0		NOTCH4	0	0	0	4	0			SDPR	0	1	0	0	0			
APOB1	4	4	4	0	0			DSTYK	0	1	2	0	1		NPF2F2	0	2	0	0	1			SDPR	0	1	0	0	0			
AHGAP25	0	1	1	0	0			DUSP19	1	0	1	0	1		NTN2	1	2	4	0	1			SDPR	0	1	0	0	0			
ARRBP19	2	1	4	0	0			EGFL6	1	0	1	0	0		NTX	1	2	4	1	1			SDPR	1	1	1	1	1			
ATP9V1C1	2	1	4	0	0		QT	EGFR	0	3	0	2	0		OR22W4	2	2	1	0	1			SDPR	1	1	3	0	0			
BHMT2	2	4	4	0	0			ELK1	2	2	0	1	0		ORC1	0	0	1	0	0			SDPR	2	0	3	0	0			
BTNA1	2	3	3	0	0			ENDOG	3	0	2	0	0		PALD	0	2	0	0	0			SDPR	2	2	3	2	0			
C17orf82	0	0	3	0	0			FAM1881	0	1	2	0	0		PDI43	1	1	0	2	0			SDPR	1	1	1	1	1			
GSX1P (C14orf120)	2	1	2	0	0			FCRL1	1	0	0	0	0		PID6	1	1	2	0	0			SDPR	1	1	1	1	1			
C15orf38	2	2	1	0	0			FORL3	1	0	0	0	0		PLD8	0	1	0	1	0			SDPR	1	1	1	1	1			
C17orf59	3	1	3	0	0			FOXO3	3	0	3	0	1		PLP	2	1	3	0	0			SDPR	3	0	3	1	0			
C17orf80	1	4	4	2	1			GLA3	4	0	3	0	0		PP1L4A	1	1	0	0	0			SDPR	3	0	3	0	0			
C19orf6 (TMEM259)	1	3	4	0	0			GPR192	2	1	2	0	0		PQDC3	3	2	2	0	0			SDPR	0	2	1	0	0			
C21orf2	2	2	3	0	0			GSX8	0	2	0	0	0		PRKDCBP	1	1	1	0	0			SDPR	1	1	1	1	1			
CGMT25 (TMEM248)	2	2	3	0	0			HHR1	2	1	2	0	0		PSAP	0	1	2	0	0			SDPR	1	1	1	1	1			
CAV1	0	3	0	0	0		A-lip, PR & QT	HMLA-DBP1	0	1	2	0	0		PSEN2	2	1	3	0	0			SDPR	2	2	3	0	0			
CAV2	1	4	2	3	0			INADL	0	4	1	0	0		PTRE	0	2	3	0	0			SDPR	1	0	0	1	0			
CAV3	1	2	1	0	0			IRF6	1	0	0	0	0		RAB7A	1	1	1	0	0			SDPR	1	1	1	0	0			
CCDC30	0	2	1	0	0			IRF7	0	1	0	0	0		RASGEF1B	0	1	0	1	0			SDPR	2	0	3	0	0			
CCDC42BP8	0	0	0	0	0			ITG88	2	2	2	0	0		RELA	1	2	2	0	0			SDPR	1	2	2	0	0			
CDH23	0	3	1	0	0			ITM2C	5	2	3	0	0		RGR	2	0	4	0	0			SDPR	2	1	3	0	0			
CHMP2A	2	3	2	0	0			KBTBD3	0	0	0	1	0		RHBD3	4	0	4	0	0			SDPR	1	1	4	0	0			
CHMP4B	4	0	4	0	0			KLRB1	0	0	0	0	0		RXP23	2	0	3	0	0			SDPR	0	2	2	0	0			
CHMP5	1	0	0	0	0			LEPROT	3	3	1	0	0		SALM1	1	1	4	0	0			SDPR	0	1	2	0	0			
CHRNA9	0	3	2	0	0			LIF	0	0	4	0	0		SCARB1	1	2	3	1	0			SDPR	1	1	1	1	1			
CLEC4A	1	3	3	3	0			LPHN3	0	0	2	1	0		SCRT1	0	1	0	0	0			SDPR	4	2	4	0	0			

Shown are the numbers of individual siRNAs targeting each gene that score positive in each screen. Green, siRNAs fulfill the assay criteria (E+H: ≥ 2 positive siRNAs / T+L: ≥ 2 positive siRNAs). Red, siRNAs does not fulfill the assay criteria (E+H: ≤ 2 positive siRNAs / T+L: ≤ 2 positive siRNAs).

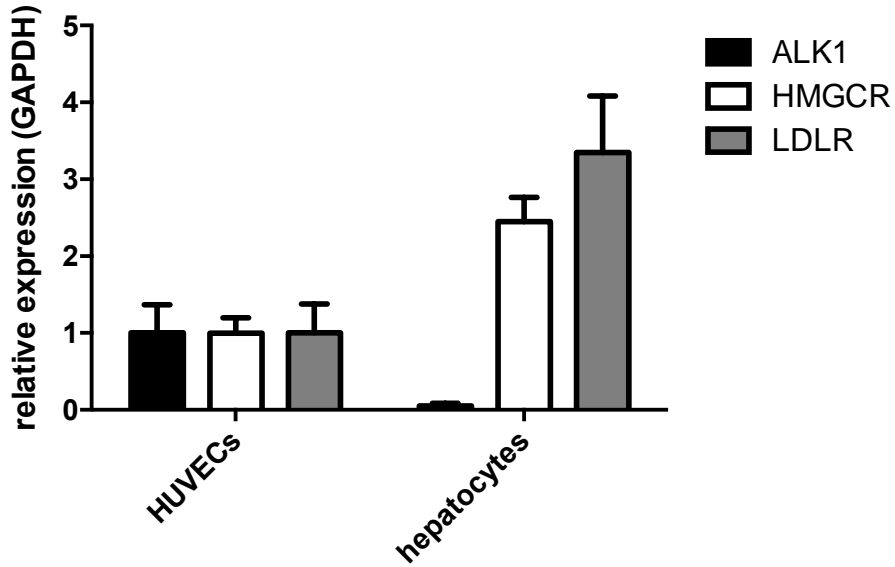
CVD	cardiovascular traits
Lipids	effect on lipids
A-rib.	atrial fibrillation
CAD	coronary artery disease
DBP	diastolic blood pressure
HDL	high-density lipoprotein
LDL	low-density lipoprotein
MAP	mean arterial pressure
PP	pulse pressure
PR	PR interval
QT	QT interval
SBP	systemic blood pressure
TC	total cholesterol
TG	triglycerid

E: DiLDL uptake in EAhy296 cells  
T: Transferrin-FTIC uptake in EAhy296 cells  
H: DiLDL uptake in HUVECs  
L: LDLR dependency  
S: endothelial specific

## Supplementary Fig. 3. Follow-up screen.

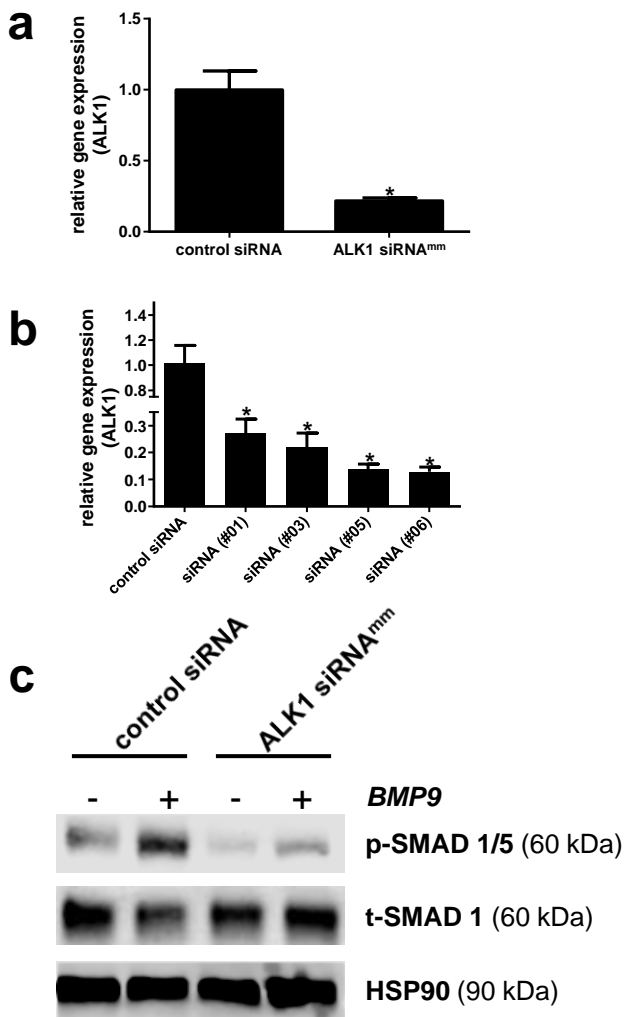
140 genes from the initial GW RNAi screen were further analysed. See Supplementary Dataset 2 for further details. References for the expression pattern are listed under Supplementary References at the end of this document. See Supplementary Dataset 3 for further details on the GWAS data.

# Supplementary Figure 4



**Supplementary Fig. 4. Transcript levels for ALK1 in human primary endothelial cells and hepatocytes**  
The transcript levels of *ACVRL1*, *HMGCR* and *LDLR* were compared between primary human endothelial cells (HUVEC) and primary human hepatocytes (healthy donors).

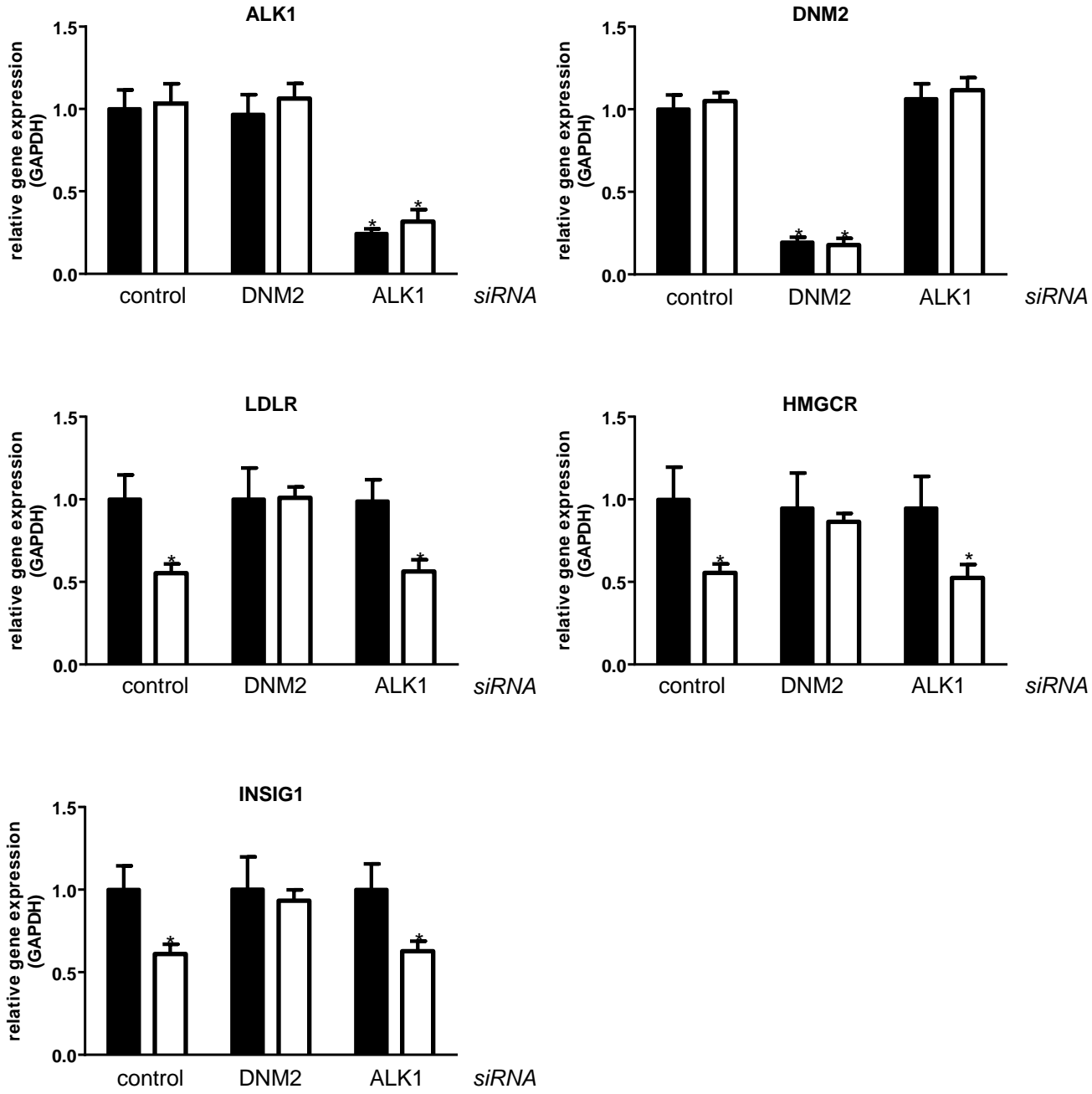
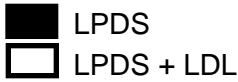
# Supplementary Figure 5



## Supplementary Fig. 5. siRNA efficiency analysis

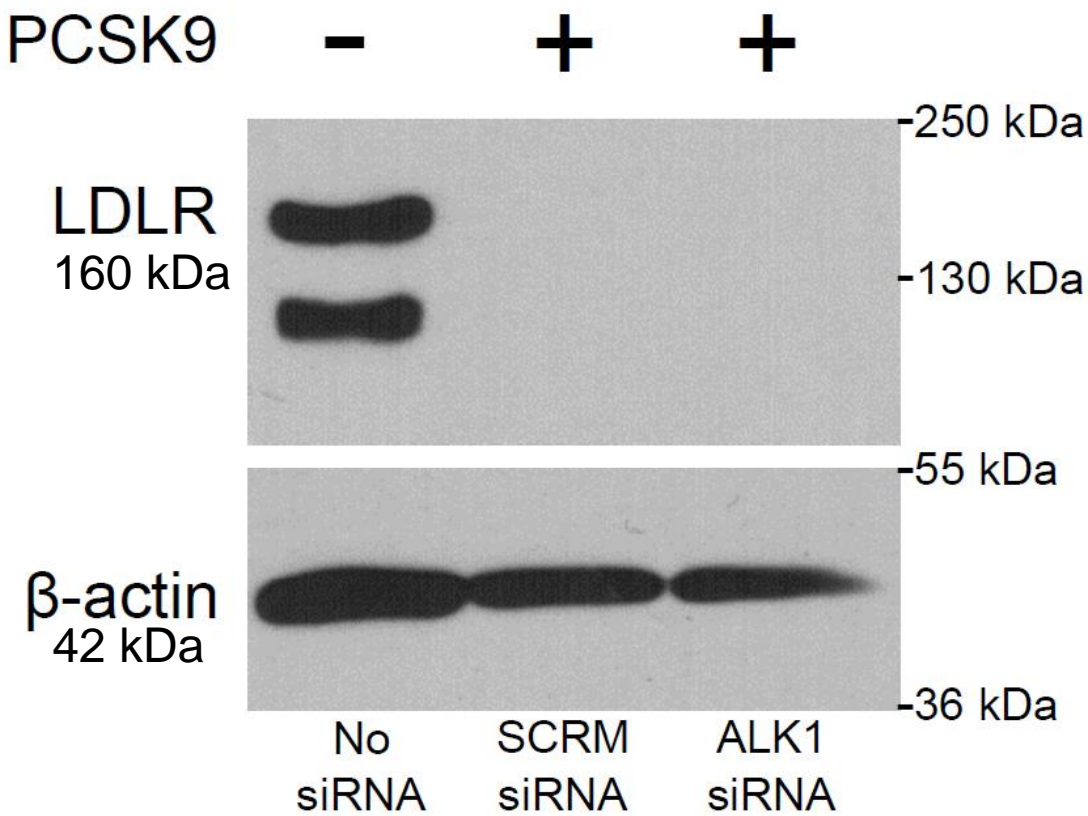
a) qPCR analysis of the knockdown efficiency of siRNA against murine ALK1 (here MLEC). Data represent the mean  $\pm$  SEM and are representative of 3 experiments in duplicate. \* $p < 0.05$ , Student's t-test. b) qPCR analysis of all 4 individual siRNAs against human ALK1 used in the GW RNAi screen. Analysis performed in HUVECs. Data represent the mean  $\pm$  SEM and are representative of 3 experiments in duplicate. \* $p < 0.05$ , Student's t-test. c) Western blot analysis of the knockdown efficiency of siRNA against murine ALK1 (here MLEC) based on the BMP9 (10 ng/ml) induced phosphorylation of SMAD 1/5. A non-cropped western blot for this experiment can be found in Supplementary Figure 12a.

# Supplementary Figure 6



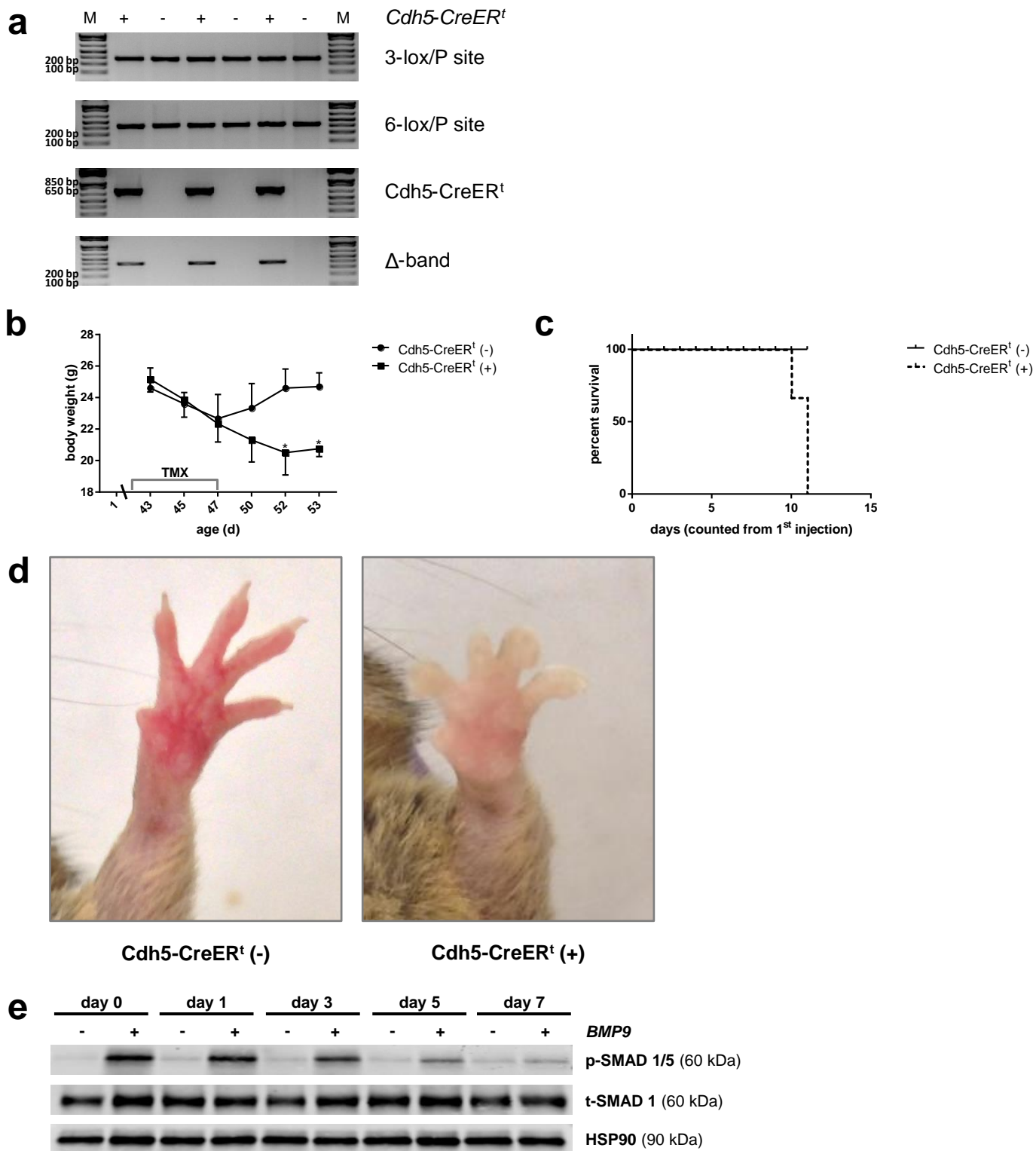
**Supplementary Fig. 6. ALK1 knockdown does not affect transcript levels of SREB2-dependent genes**  
 Cells were treated with control siRNA, *ACVRL1* siRNA and *DNM2* siRNA and kept in either low LDL media (LPDS) or high LDL media (LDL pretreated), before transcripts for genes involved in sterol sensing were analysed. Data represent the mean  $\pm$  SEM and are representative of 3 experiments in duplicate. \*p < 0.05, Student's t-test.

# Supplementary Figure 7



**Supplementary Fig. 7. PCSK9 conditioned media leads to degradation of LDLR in HCAECs**  
Treatment of HCAECs transfected with control siRNA or *ACVRL1* siRNA with PCSK9 conditioned media for at least 6 hrs results in a complete removal of LDLR.

# Supplementary Figure 8

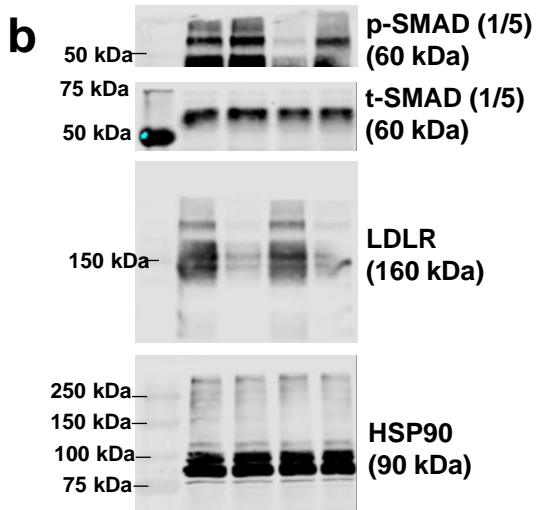
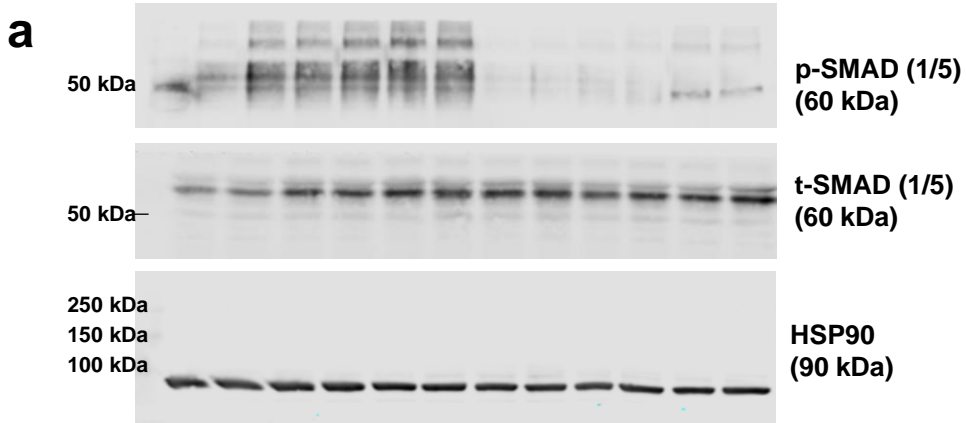


## Supplementary Fig. 8. Endothelial specific deletion of ALK1 in adult mice leads to rapid death

a) Genotyping results of *Acvrl<sup>fl/fl</sup>* mice with or without the inducible *Cdh5-CreERT2* transgene 7 days after first TMX injection. b) Weight measurements. Data represent the mean  $\pm$  SEM and are representative of 3 animals each. \* $p < 0.05$ , Student's t-test. c) Kaplan-Meier curve. d) Representative images of paws from Cre-negative and Cre-positive animals 7 days after the first TMX injection. e) Cre-positive animals were injected with TMX for 0, 1, 3, 5 or 7 days and primary MLECs were isolated and treated after 3 hrs of starvation with vehicle or BMP9 (10 ng/ml). A non-cropped western blot for this experiment can be found in Supplementary Figure 12b.



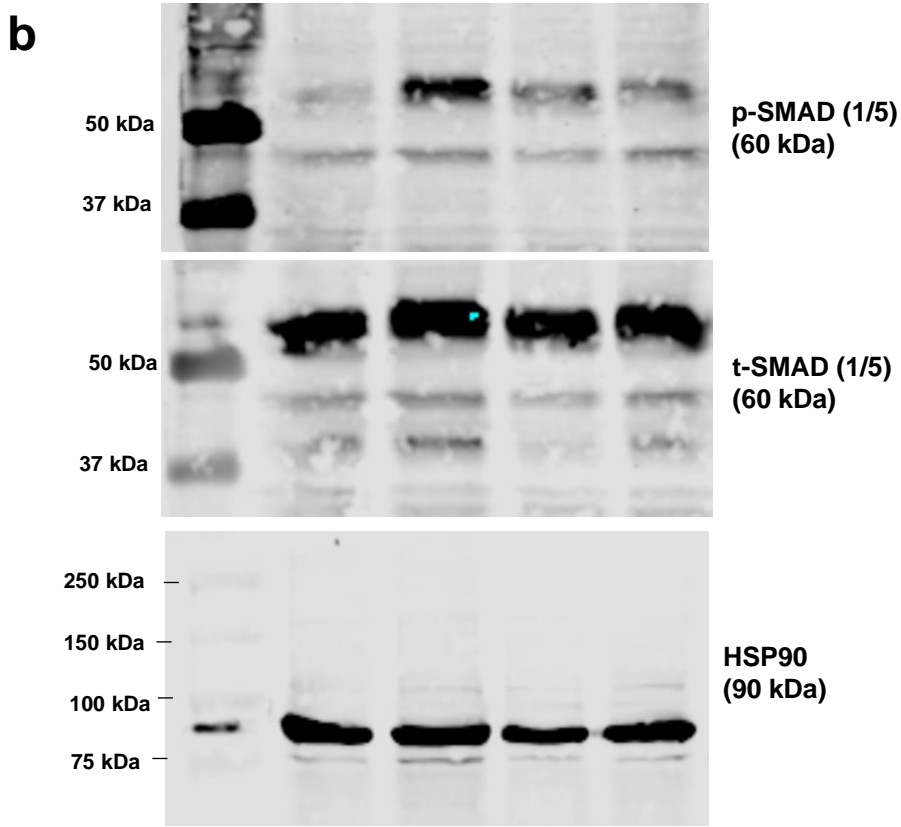
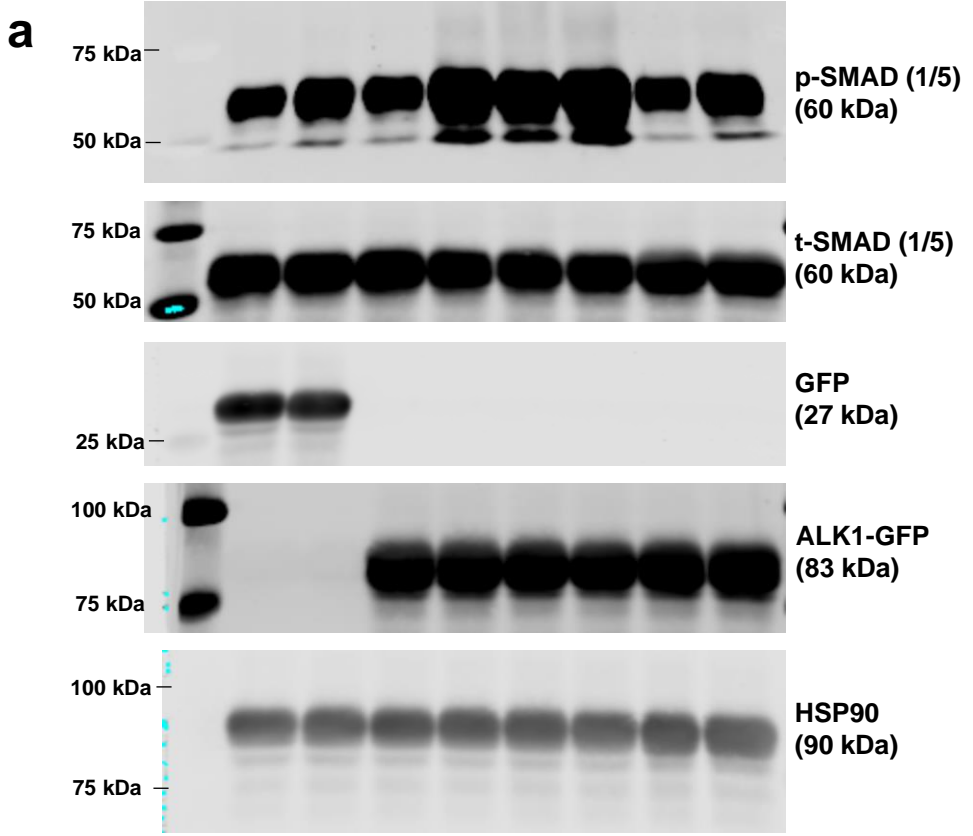
# Supplementary Figure 9



**Supplementary Fig. 9. Original Western Blots**

a) Original gel scans for Fig. 2b. b) Original gel scans for Fig. 3b.

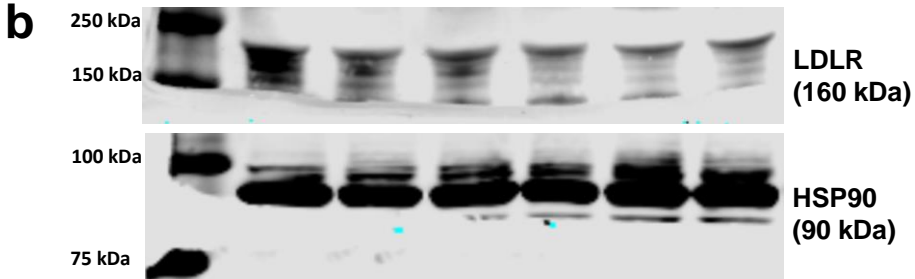
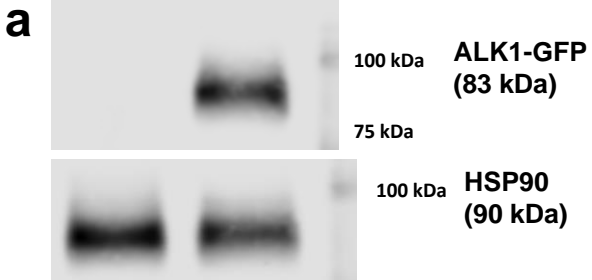
# Supplementary Figure 10



**Supplementary Fig. 10. Original Western Blots**

a) Original gel scans for Fig. 4c. b) Original gel scans for Fig. 4e.

# Supplementary Figure 11

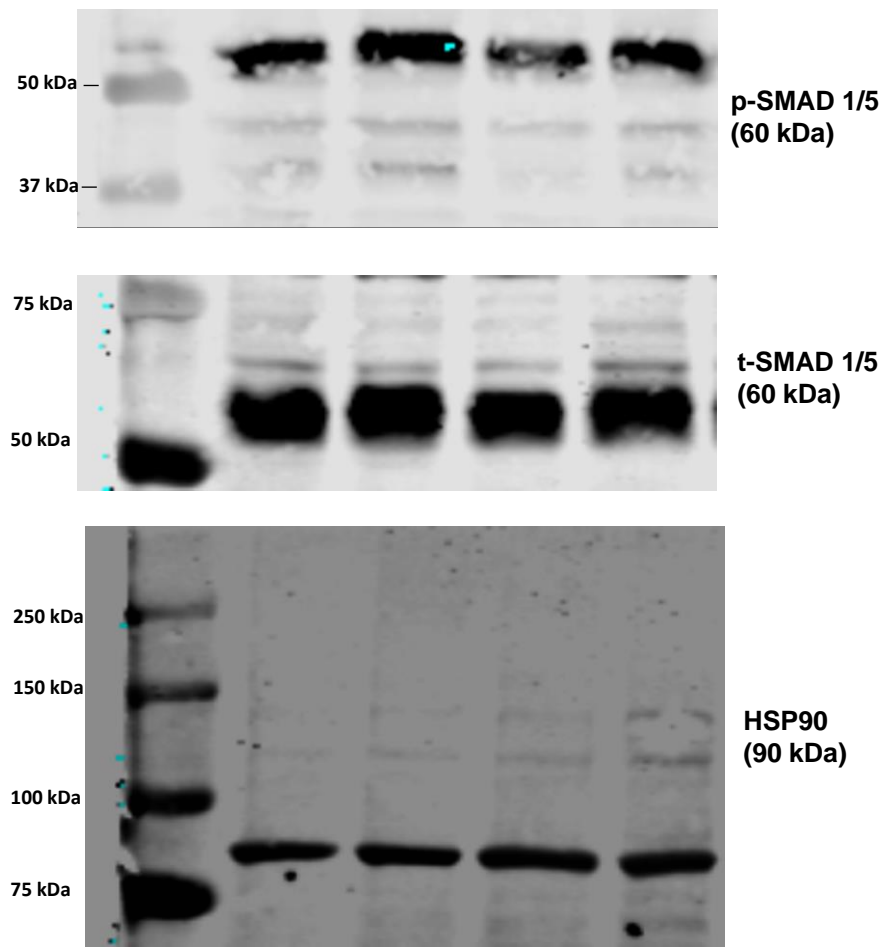


**Supplementary Fig. 11. Original Western Blots**

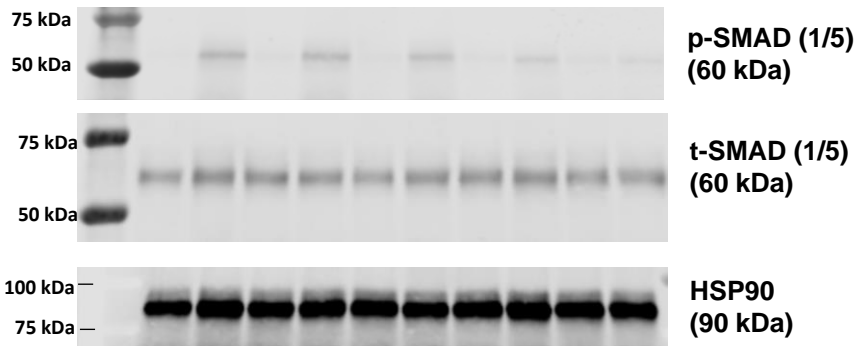
a) Original gel scans for Fig. 5a. b) Original gel scans for Sup. Fig. 1b.

# Supplementary Figure 12

**a**



**b**



**Supplementary Fig. 12. Original Western Blot**

a) Original gel scans for Sup. Fig. 6c. b) Original gel scans for Sup. Fig. 9e.

# Supplementary Table 1

Network 1	Network 2	Network 3
Hereditary Disorder, Metabolic Disease, Neurological Disease	Carbohydrate Metabolism, Lipid Metabolism, Small Molecule Biochemistry	Cancer, Carbohydrate Metabolism, Cell Cycle
<b>ACVRL1</b> , Akt, <b>ANGPT4</b> , <b>ATP6V1C1</b> , caspase, <b>CX3CR1</b> , <b>ENDOG</b> , ERK, ERK1/2, <b>FXYD3</b> , Gpcr, GPR111, GPR144, GPR152, GPR162, GPR174, <b>GPR182</b> , Insulin, <b>LIF</b> , <b>MAPK6</b> , <b>NAPA</b> , NFkB (complex), P38 <b>MAPK6</b> , <b>PSEN2</b> , <b>RGR</b> , <b>RHBDD3</b> , RXFP3, <b>SDC1</b> , Secretase gamma, <b>SLC38A3</b> , <b>SRP72</b> , <b>SYT9</b> , <b>TRPC6</b> , Vegf, VN1R2	<b>AP2M1</b> , <b>ARHGAP9</b> , ARL17A, ATG4D, <b>C17orf59</b> , CCDC94, <b>CHMP4B</b> , DYNLL1, FAHD2A, FAM216A, GDAP2, <b>GJA3</b> , <b>GSKIP</b> , <b>HLA-QB1</b> , HNF4A, <b>MIEF2</b> , <b>MRGPRE</b> , MTRF1L, ORMDL2, PAX6, phosphatidylserin, <b>PLLP</b> , RNF44, SLC35D1, SLC7A6OS, SNX11, <b>SUPT5H</b> , <b>SYS1</b> , <b>SYTL2</b> , TMUB2, <b>TREML2</b> , TTC26, UBC, ZNF222, ZNF586	IL2, <b>TSPAN32</b>

## Supplementary Table 1. Qiagen's Ingenuity Pathway Analysis.

Analysis of the 34 gene hits revealed 3 distinct networks. Representation in a table format. Genes in bold were found in the screen and genes in red cluster in the vesicular trafficking pathway.

## Supplementary Table 2

gene	ordering number	company	concentration
control siRNA	D-001220-01	Dharmacon	20 nM
scamble control siRNA	1027310	Qiagen	20 nM
ALK1 siRNA (human)	D-005302-06	Dharmacon	20 nM
ALK1 siRNA (murine)	M-043004-01	Dharmacon	20 nM
DNM2 siRNA (human)	customized target sequence: 5' - AACATGCCGAGTTTTTGCCT - 3'	Qiagen	20 nM
LDLR siRNA (human)	4392420 / ID: s224006	Ambion	20 nM
LDLR shRNAs lentiviral knockdown (human)	TRCN0000056517 5' - CCGGACAGAGGATGAGGTCCACATTCTCGAGAAT GTGGACCTCATCCTCTGTTTTTTG-3'	Sigma-Aldrich	n/a
	TRCN0000262146 5' - CCGGGGGCGACAGATGCGAAAGAACTCGAGTTT CTTTCGCATCTGTCGCCCTTTTTG-3'		
	TRCN0000262148 5' - CCGGACATCAACAGCATCAACTTTGCTCGAGCAA AGTTGATGCTGTTGATGTTTTTTG-3'		
	TRCN0000262149 5' - CCGGATGGAAGAACTGGCGGCTTAACTCGAGTTA AGCCGCCAGTTCTTCCATTTTTTTG-3'		
	TRCN0000282124 5' - CCGGGATGAAGTTGGCTGCGTTAATCTCGAGATT AACGCAGCCAACCTTCATCTTTTTG-3'		
NPC2 siRNA (human)	M-017216-00	Dharmacon	20 nM

# Supplementary Table 3

protein	ordering number	company	working concentration
<b>Western Blot</b>			
$\beta$ -actin	sc-47778	Santa Cruz	1 : 1,000
HSP90	sc-13119	Santa Cruz	1 : 1,000
GFP	sc-8664	Santa Cruz	1 : 1,000
LDLR	10007665	Cayman	1 : 500
p-SMAD 1/5 (S463/S465)	9516	Cell Signaling	1 : 500
t-SMAD 1	9743	Cell Signaling	1 : 1,000
<b>FACS</b>			
LDLR	sc-18823	Santa Cruz	1.5 $\mu$ g/tube
mmlgG2b	sc-3879	Santa Cruz	1.5 $\mu$ g/tube
Goat anti-Mouse IgG (H+L) Secondary Antibody, Alexa Fluor® 488 conjugate	A-11001	Invitrogen	1:500
<b>Immunofluorescence</b>			
EEA1	610456	BD Transduction Laboratories	1:200
<b>MLEC isolation</b>			
M-450 Dynabeads conjugated with sheep anti-rat IgG	110.07	Dynal Biotech	50 $\mu$ l beads/6 $\mu$ l antibody
Affinity-purified anti-mouse CD31 (PECAM-1) antibody	553370	Pharmingen	6 $\mu$ l antibody/3 mice

# Supplementary Table 4

Cdh5-CreERT2		
forward	5'-GCC TGC ATT ACC GGT CGA TGC AAC GA-3'	
reverse	5'-GTG GCA GAT GGC GCG GCA ACA CCA TT-3'	
amplicon size	700 bp	
PCR program		
step 1	93°C	2:00 min
step 2	93°C	0:30 min
step 3	67°C	0:30 min
step 4	72°C	0:45 min
step 5	go to 2, 35 x	
step 6	72°C	10:00 min
step 7	4°C	forever

LDLR-KO		
P1 (common)	5'-CCA TAT GCA TCC CCA GTC TT-3'	
P2 (WT)	5'-GCG ATG GAT ACA CTC ACT GC-3'	
P3 (Neo)	5'- AAT CCA TCT TGT TCA ATG GCC GAT C-3'	
WT	167 bp	
KO	350 bp	
Het	167 bp + 350 bp	
PCR program		
step 1	95°C	3:00 min
step 2	95°C	0:10 min
step 3	61°C	0:45 min
step 4	72°C	3:00 min
step 5	go to 2, 35 x	
step 6	72°C	10:00 min
step 7	4°C	forever

ALK1 floxed allele		
forward loxP 3	5'-CAG CAC CTA CAT CTT GGG TGG AGA-3'	
reverse loxP 3	5'-ACT GTT CTT CCT CGG AGC CTT GTC-3'	
amplicon size floxed	> 300 bp	
amplicon size unfloxed	187 bp	
forward loxP 6	5'-CCT GGA CAG CGA CTG TAC TAC-3'	
reverse loxP 6	5'-GCC CCA TTG CTC TCC TCA AA-3'	
amplicon size floxed	> 400 bp	
amplicon size unfloxed	356 bp	
By using forward loxP 3 and reverse loxP 6 primers the $\Delta$ -band after Cre-recombinase excision can be detected (~ 400 bp).		
PCR program		
step 1	94°C	10:00 min
step 2	94°C	0:30 min
step 3	60°C	0:40 min
step 4	72°C	0:40 min
step 5	go to 2, 34 x	
step 6	72°C	2:00 min
step 7	4°C	forever



# Supplementary Table 5

gene	species	primers (5'→3')	
		forward	reverse
ALK1	human	CGAGGGATGAACAGTCCTGG	GTCATGTCTGAGGCGATGAAG
	murine	GGGCCTTTTGATGCTGTCG	TGGCAGAATGGTCTCTTGCAAG
DNM2	human	GTTTGTGCTGACTGCCGAGT	TTCCAGCTGTCCACGTCTTC
GAPDH	human	CTCTCTGCTCCTCCTGTTGAC	TGAGCGATGTGGCTCGGCT
	murine	AATGTGTCCGTCGTGGATCTGA	AGTGTAGCCCAAGATGCCCTTC
HMGCR	human	TGATTGACCTTTCCAGAGCAAG	CTAAAATTGCCATTCCACGAGC
INSIG1	human	GCACTGCATTAAACGTGTGG	GCAGCACTGAAATGAATGGA
LDLR	human	TCTGCAACATGGCTAGAGACT	TCCAAGCATTGTTGGTCCC
PCSK9	human	GGAGCTGGCCTTGAAGTTGCC	ACCGTGGAGGGGTAATCCGC

# Supplementary References

1. Larrivee B, Prahst C, Gordon E, del Toro R, Mathivet T, Duarte A, Simons M, Eichmann A. Alk1 signaling inhibits angiogenesis by cooperating with the notch pathway. *Developmental Cell*. 2012;22:489-500
2. Lee HJ, Cho CH, Hwang SJ, Choi HH, Kim KT, Ahn SY, Kim JH, Oh JL, Lee GM, Koh GY. Biological characterization of angiopoietin-3 and angiopoietin-4. *FASEB journal : official publication of the Federation of American Societies for Experimental Biology*. 2004;18:1200-1208
3. Meng J, Wang J, Lawrence GW, Dolly JO. Molecular components required for resting and stimulated endocytosis of botulinum neurotoxins by glutamatergic and peptidergic neurons. *FASEB journal : official publication of the Federation of American Societies for Experimental Biology*. 2013
4. Takefuji M, Asano H, Mori K, Amano M, Kato K, Watanabe T, Morita Y, Katsumi A, Itoh T, Takenawa T, Hirashiki A, Izawa H, Nagata K, Hirayama H, Takatsu F, Naoe T, Yokota M, Kaibuchi K. Mutation of arhgap9 in patients with coronary spastic angina. *Journal of human genetics*. 2010;55:42-49
5. Feng S, Deng L, Chen W, Shao J, Xu G, Li YP. Atp6v1c1 is an essential component of the osteoclast proton pump and in f-actin ring formation in osteoclasts. *The Biochemical journal*. 2009;417:195-203
6. Hundsrucker C, Skroblin P, Christian F, Zenn HM, Popara V, Joshi M, Eichhorst J, Wiesner B, Herberg FW, Reif B, Rosenthal W, Klussmann E. Glycogen synthase kinase 3beta interaction protein functions as an a-kinase anchoring protein. *J Biol Chem*. 2010;285:5507-5521
7. The Human Protein Atlas.  
Uhlen M, Fagerberg L, Hallstrom BM, Lindskog C, Oksvold P, Mardinoglu A, Sivertsson A, Kampf C, Sjostedt E, Asplund A, Olsson I, Edlund K, Lundberg E, Navani S, Szigartyo CA, Odeberg J, Djureinovic D, Takanen JO, Hober S, Alm T, Edqvist PH, Berling H, Tegel H, Mulder J, Rockberg J, Nilsson P, Schwenk JM, Hamsten M, von Feilitzen K, Forsberg M, Persson L, Johansson F, Zwahlen M, von Heijne G, Nielsen J, Ponten F. Proteomics. Tissue-based map of the human proteome. *Science*. 2015;347:1260419
8. Martinelli N, Hartlieb B, Usami Y, Sabin C, Dordor A, Miguet N, Avilov SV, Ribeiro EA, Jr., Gottlinger H, Weissenhorn W. Cc2d1a is a regulator of escrt-iii chmp4b. *J Mol Biol*. 2012;419:75-88
9. Hochheiser K, Heuser C, Krause TA, Teteris S, Ilias A, Weisheit C, Hoss F, Tittel AP, Knolle PA, Panzer U, Engel DR, Tharaux PL, Kurts C. Exclusive cx3cr1 dependence of kidney dcs impacts glomerulonephritis progression. *The Journal of clinical investigation*. 2013;123:4242-4254
10. McDermott-Roe C, Ye J, Ahmed R, Sun XM, Serafin A, Ware J, Bottolo L, Muckett P, Canas X, Zhang J, Rowe GC, Buchan R, Lu H, Braithwaite A, Mancini M, Hauton D, Marti R, Garcia-Arumi E, Hubner N, Jacob H, Serikawa T, Zidek V, Papousek F, Kolar F, Cardona M, Ruiz-Meana M, Garcia-Dorado D, Comella JX, Felkin LE, Barton PJ, Arany Z, Pravenec M, Petretto E, Sanchis D, Cook SA. Endonuclease g is a novel determinant of cardiac hypertrophy and mitochondrial function. *Nature*. 2011;478:114-118
11. Bibert S, Roy S, Schaer D, Felley-Bosco E, Geering K. Structural and functional properties of two human fxyd3 (mat-8) isoforms. *J Biol Chem*. 2006;281:39142-39151
12. Li L, Cheng C, Xia CH, White TW, Fletcher DA, Gong X. Connexin mediated cataract prevention in mice. *PLoS One*. 2010;5
13. Xiao L, Harrell JC, Perou CM, Dudley AC. Identification of a stable molecular signature in mammary tumor endothelial cells that persists in vitro. *Angiogenesis*. 2014;17:511-518
14. Griffioen M, van der Meijden ED, Slager EH, Honders MW, Rutten CE, van Luxemburg-Heijs SA, van dem Borne PA, van Rood JJ, Willemze R, Falkenburg JH. Identification of phosphatidylinositol 4-kinase type ii beta as hla class ii-restricted target in graft versus leukemia reactivity. *Proc Natl Acad Sci U S A*. 2008;105:3837-3842
15. Liu SC, Tsang NM, Chiang WC, Chang KP, Hsueh C, Liang Y, Juang JL, Chow KP, Chang YS. Leukemia inhibitory factor promotes nasopharyngeal carcinoma progression and radioresistance. *The Journal of clinical investigation*. 2013;123:5269-5283
16. Seternes OM, Mikalsen T, Johansen B, Michaelsen E, Armstrong CG, Morrice NA, Turgeon B, Meloche S, Moens U, Keyse SM. Activation of mk5/prak by the atypical map kinase erk3 defines a novel signal transduction pathway. *The EMBO journal*. 2004;23:4780-4791
17. Cox PJ, Pitcher T, Trim SA, Bell CH, Qin W, Kinloch RA. The effect of deletion of the orphan g - protein coupled receptor (gpcr) gene mrge on pain-like behaviours in mice. *Molecular pain*. 2008;4:2

# Supplementary References (*continuation*)

18. Ferland RJ, Batiz LF, Neal J, Lian G, Bundock E, Lu J, Hsiao YC, Diamond R, Mei D, Banham AH, Brown PJ, Vanderburg CR, Joseph J, Hecht JL, Folkerth R, Guerrini R, Walsh CA, Rodriguez EM, Sheen VL. Disruption of neural progenitors along the ventricular and subventricular zones in periventricular heterotopia. *Human molecular genetics*. 2009;18:497-516
19. Miller AD, Bergholz U, Ziegler M, Stocking C. Identification of the myelin protein plasmolipin as the cell entry receptor for mus caroli endogenous retrovirus. *J Virol*. 2008;82:6862-6868
20. Rivabene R, Visentin S, Piscopo P, De Nuccio C, Crestini A, Svetoni F, Rosa P, Confaloni A. Thapsigargin affects presenilin-2 but not presenilin-1 regulation in sk-n-be cells. *Experimental biology and medicine*. 2013
21. Ksantini M, Senechal A, Bocquet B, Meunier I, Brabet P, Hamel CP. Screening genes of the visual cycle rgr, rbp1 and rbp3 identifies rare sequence variations. *Ophthalmic genetics*. 2010;31:200-204
22. Liu J, Liu S, Xia M, Xu S, Wang C, Bao Y, Jiang M, Wu Y, Xu T, Cao X. Rhomboid domain-containing protein 3 is a negative regulator of tlr3-triggered natural killer cell activation. *Proc Natl Acad Sci U S A*. 2013;110:7814-7819
23. Bathgate RA, Halls ML, van der Westhuizen ET, Callander GE, Kocan M, Summers RJ. Relaxin family peptides and their receptors. *Physiological reviews*. 2013;93:405-480
24. Szatmari T, Dobra K. The role of syndecan-1 in cellular signaling and its effects on heparan sulfate biosynthesis in mesenchymal tumors. *Frontiers in oncology*. 2013;3:310
25. Jenstad M, Chaudhry FA. The amino acid transporters of the glutamate/gaba-glutamine cycle and their impact on insulin and glucagon secretion. *Frontiers in endocrinology*. 2013;4:199
26. Liu T, Yu R, Jin S-B, Han L, Lendahl U, Zhao J, Nistér M. The mitochondrial elongation factors mief1 and mief2 exert partially distinct functions in mitochondrial dynamics. *Experimental Cell Research*. 2013;319:2893-2904
27. Kirwan M, Walne Amanda J, Plagnol V, Velangi M, Ho A, Hossain U, Vulliamy T, Dokal I. Exome sequencing identifies autosomal-dominant srp72 mutations associated with familial aplasia and myelodysplasia. *The American Journal of Human Genetics*. 2012;90:888-892
28. Wier AD, Mayekar MK, Heroux A, Arndt KM, VanDemark AP. Structural basis for spt5-mediated recruitment of the paf1 complex to chromatin. *Proc Natl Acad Sci U S A*. 2013;110:17290-17295
29. Setty SR, Strochlic TI, Tong AH, Boone C, Burd CG. Golgi targeting of arf-like gtpase arl3p requires its alpha-acetylation and the integral membrane protein sys1p. *Nature cell biology*. 2004;6:414-419
30. Iezzi M, Eliasson L, Fukuda M, Wollheim CB. Adenovirus-mediated silencing of synaptotagmin 9 inhibits ca<sup>2+</sup>-dependent insulin secretion in islets. *FEBS Letters*. 2005;579:5241-5246
31. Ménasché G, Ménager MM, Lefebvre JM, Deutsch E, Athman R, Lambert N, Mahlaoui N, Court M, Garin J, Fischer A, de Saint Basile G. A newly identified isoform of slp2a associates with rab27a in cytotoxic t cells and participates to cytotoxic granule secretion. *Blood*. 2008;112:5052-5062
32. Allcock RJ, Barrow AD, Forbes S, Beck S, Trowsdale J. The human trem gene cluster at 6p21.1 encodes both activating and inhibitory single igv domain receptors and includes nkp44. *European journal of immunology*. 2003;33:567-577
33. Seo K, Rainer PP, Shalkey Hahn V, Lee D-i, Jo S-H, Andersen A, Liu T, Xu X, Willette RN, Lepore JJ, Marino JP, Birnbaumer L, Schnackenberg CG, Kass DA. Combined trpc3 and trpc6 blockade by selective small-molecule or genetic deletion inhibits pathological cardiac hypertrophy. *Proceedings of the National Academy of Sciences*. 2014
34. Gartlan KH, Belz GT, Tarrant JM, Minigo G, Katsara M, Sheng K-C, Sofi M, van Spriel AB, Apostolopoulos V, Plebanski M, Robb L, Wright MD. A complementary role for the tetraspanins cd37 and tssc6 in cellular immunity. *The Journal of Immunology*. 2010;185:3158-3166